Defense Technical Information Center Compilation Part Notice

ADP011162

TITLE: Predicton of Combustion-Driven Dynamic Instability for High Performance Gas Turbine Combustors: Part I

DISTRIBUTION: Approved for public release, distribution unlimited

This paper is part of the following report:

TITLE: Active Control Technology for Enhanced Performance Operational Capabilities of Military Aircraft, Land Vehicles and Sea Vehicles [Technologies des systemes a commandes actives pour l'amelioration des performances operationnelles des aeronefs militaires, des vehicules terrestres et des vehicules maritimes]

To order the complete compilation report, use: ADA395700

The following component part numbers comprise the compilation report:
ADP011101 thru ADP011178

Click here to view PowerPoint presentation; Press Esc to exit

Prediction of Combustion-Driven Dynamic Instability For High Performance Gas Turbine Combustors: Part I

B. Sekar
Turbine Engine Division
Air Force Research Laboratory
Room D 138, Building 18
1950 5th Street
Wright-Patterson AFB, OH 45433

M. A. Mawid & T. W. Park
Engineering Research and Analysis Company
Wright-Patterson AFB, OH 45433, USA

S. Menon
Department of Aerospace Engineering
Georgia Institute of Technology
Atlanta, GA 30332, USA

ABSTRACT

This paper describes the development and application of a combined detailed three-dimensional large eddy simulation (LES) and one-dimensional analysis tool to predict and actively control combustion-driven dynamic instabilities in gas turbine combustors. The integration of detailed finite-rate kinetics into LES and use of In-situ Adaptive Tabulation (ISAT) to efficiently calculate multi-species finite-rate kinetics in LES along with the use of global kinetics in the one-dimensional analysis tool was demonstrated. The results showed that LES can be effectively used to simulate complex reacting flows in gas turbine combustors and to identify regions of combustion instabilities. The results also showed that the one-dimensional combustor analysis with global kinetics can then be used both to capture the combustor unstable modes of the predicted regions of instabilities and to actively control these instabilities. In particular, the results demonstrated that by modulating the primary fuel injection rates and the time-lag between the instant of fuel-air mixture injection and heat release, damping out the instabilities may be achieved.

NOMENCLATURE

a^* = Reference speed of sound
D = Diffusion coefficient
K_0 = Reaction rate constant
k = Bulk modulus of the fluid
L = Combustor length
$\dot{m}$ = Fuel-air mixture injection rate
Pr_t = Turbulent Prandtl number, $\mu_t c_p / k_t$
p = Non-dimensional pressure, $\bar{p}/p^*$
p^* = Reference pressure
p' = Combustor pressure fluctuations
Q_{fh} = Heat transferred from/to the flameholder
q_0 = Heat of reaction
R = Non-dimensional reaction rate
Re^* = Reference Reynolds number, $\rho^* a^* L/\mu$
Sc_t = Turbulent Schmidt number, ν/D
T = Non-dimensional temperature, $\bar{T}/T^*$
T^* = Reference temperature
T_i = Non-dimensional temperature in the i^{th} numerical cell
T_i^{fh} = Non-dimensional temperature at the flameholder location
T_{ign} = Non-dimensional ignition temperature
t = Non-dimensional time, $\bar{t}/t^*$
t^* = Reference time, L/a^*
u = Non-dimensional axial velocity, $\bar{u}/a^*$
V = Volume of the fuel feed system
x = Non-dimensional distance, $\bar{x}/L$
y_i = Mass fraction of i^{th} species

Greek Letters

α = User specified constant in Eq. (7)
ε_t = Turbulent to laminar viscosity ratio, μ_t/μ
ϕ = Equivalence ratio

Paper presented at the RTO AVT Symposium on "Active Control Technology for Enhanced Performance Operational Capabilities of Military Aircraft, Land Vehicles and Sea Vehicles", held in Braunschweig, Germany, 8-11 May 2000, and published in RTO MP-051.

γ = Specific heat ratio, c_p/c_v
μ = Molecular viscosity
μ_t = Turbulent viscosity
ρ = Non-dimensional density, $\overline{\rho}/\rho^*$
ρ^* = Reference density
ω = Non-dimensional fuel pulsation frequency

Superscripts

* = Reference quantities
– = Dimensional quantities

Subscripts

o = Total quantities

1 INTRODUCTION

The Air Force Integrated High Performance Turbine Engine Technology (IHPTET) combustors must operate free of combustion-driven dynamic instabilities that could compromise the structural integrity of high performance engines. To double the thrust to weight ratio, as required for future high performance military engines, the combustor will be required to operate at much higher overall design equivalence ratios, P3 and T3 than the existing military aircraft engines combustors. In addition, weight reductions in the combustor, diffuser and fuel injectors can be only achieved through innovative integration and packaging of these components. Therefore, combustor, diffuser and fuel injectors must be designed in a manner that will lead to instability-free (or substantially damped instabilities) operation. Active combustion control techniques may also be implemented to damp instabilities. While the active control technology attempts to introduce an out of phase disturbance with the combustor pressure acoustics, the passive control technology requires a profound understanding of the various driving mechanisms such as air and fuel flows variations, unsteady heat release and their interaction that cause combustion instabilities.

Most existing combustors design databases lack a provision for predicting combustion-driven instabilities during the predesign and design phases. Currently, a need exists to predict and quantify combustion instabilities in high performance military combustors. Axial, tangential and radial instability modes may all develop in the combustors that could severely impact the engine performance and its structural integrity. Various approaches are presently used to predict combustion instabilities. These approaches range from one-dimensional linear stability-based [1-3], to one, two and three-dimensional non-linear-CFD-based [4-8]. Mohanraj et. al. [5] developed a one-dimensional combustor model using a heuristic mixing model along with a semi empirical open loop active controller. Quinn and Paxson [9] used a one-dimensional model to study thermo-acoustic instabilities in combustion systems. Other analytical models [10-11] based upon the unsteady-pressure wave equation in three-dimensions were also developed and calibrated/anchored to experimental results under controlled conditions such that extrapolation to other conditions can be performed.

In LES modeling of the momentum transport scales larger than the grid size are computed using a time- and space-accurate scheme, while the effect of the unresolved smaller scales (assumed to be mostly isotropic) on the resolved motion is modeled using an eddy viscosity based subgrid model. This approach is acceptable for momentum transport since all the energy containing scales are resolved and all the unresolved scales (that primarily provide for dissipation of the energy transferred from the large scales) can be modeled by using an eddy dissipation subgrid model. However, these arguments cannot be extended to reacting flows since , for combustion to occur, fuel and oxidizer species must mix at the molecular level. Since, this process is dominated by the mixing process in the small-scales, ad hoc eddy diffusivity concepts cannot be used except under very specialized conditions. To deal with these distinctly different modeling requirements, a new subgrid mixing and combustion model has been developed that allows for proper resolution of the small scale scalar mixing and combustion effects within the framework of a conventional LES approach.

The earlier studies [12, 13] have established the ability of the LES model in premixed combustion and in fuel-air mixing. To reduce the computational cost, the past calculations employed flamelet models (for premixed combustion) or simulated fuel-air mixing without detailed chemical kinetics. However, for realistic simulations for the reacting flow, detailed finite-rate kinetics must be used, especially if pollutant formation is to be studied. As is well known, the computational effort involved when using detailed kinetics is so large as to make LES of even a simple configuration computationally infeasible. Typically, global kinetics are employed to reduce the computational cost. However, such kinetics are not able to deal with ignition and extinction processes and are also unable to accurately predict pollutant (No_x, CO and UHC) formation.

Due to the limited data available on combustion-driven instability for gas turbine combustors, no consensus as to what approach should be used to predict instabilities during the diffuser/fuel injectors/combustor predesign and development stages yet exists. The primary objective of this study is to demonstrate the application of a combined large eddy simulation and an unsteady one-dimensional combustor model approach for predicting the combustor's unstable modes and for

investigating the effectiveness of the fuel flow modulation methodology to actively control and suppress the combustor's instabilities. The present study is considered work-in-progress towards using LES along with a simpler analysis tool to predict instabilities at the pre-design and design stages of gas turbine combustors. The paper is organized as follows. The LES model formulation along with its numerical implementation is presented in the next section, followed by sections on the governing equations and combustion model for the one-dimensional combustor analysis tool and results. The final section is the conclusion.

2 LES MODEL

The compressible LES equations are obtained by Favre-filtering Navier-Stokes equations using a top-hat filter (appropriate for finite-volume schemes). The filtering process results in terms in the resolved LES equations that require modeling. The final LES equations are avoided here for brevity since they are described elsewhere [14]. In general, the subgrid terms representing the subgrid stress tensor, the subgrid heat flux, the subgrid viscous work, the subgrid species mass flux, and the subgrid enthalpy flux all require modeling.

The subgrid stresses in the LES momentum equations are modeled using an eddy viscosity, which in turn, is modeled in terms of the LES filter width Δ and the subgrid kinetic energy K^{sgs}. A transport model equation for the subgrid kinetic energy is solved along with the other LES equations. The effects of subgrid turbulence on flame structure (and propagation) in premixed combustion can be quantified in terms of the subgrid kinetic energy and thus, it is advantageous to use this type of LES model for reacting flows. Another distinct advantage of this approach is that this model does not assume equilibrium between subgrid kinetic energy production and dissipation (implicit in algebraic models) and thus, helps to attribute a relaxation time associated with the nonequilibrium in the subgrid scales.

To handle the distinctly different physics of scalar mixing and chemical reactions a new subgrid model has been developed. Details of this model have been reported elsewhere [12, 13] and therefore, only summarized here. This model is called Linear Eddy Model (LEM) [15].

2.1 LEM MODEL FORMULATION

The details of the LEM model have been given elsewhere [15] and therefore, are only briefly summarized here. LEM is a stochastic model, which treats reaction-diffusion and turbulent convection separately but concurrently. Reaction-diffusion processes evolve on a one-dimensional (1D) domain in which all the characteristic length scales in the turbulent field (from L to η) are fully resolved (6 cells are used to resolve η). The orientation of the 1D domain is in the direction of the scalar gradient and within this domain, the equations governing constant pressure, adiabatic laminar flame propagation are solved. The deterministic simulation of the reaction-diffusion processes can be viewed as a local direct numerical simulation. As a result, the reaction rate terms do not require any closure.

Turbulent stirring of the scalar field is implemented as distinctly independent process that interrupts the deterministic evolution of the reaction-diffusion processes on the 1D domain. Stirring is implemented as stochastic re-arrangement events called triplet maps, each of which represents the action of a turbulent eddy on the scalar fields. It has been shown that this mapping can capture correctly the physical increase in scalar gradient (without affecting the mean scalar concentration) due to eddy motion. Three parameters are needed to implement these turbulent stirring events: the typical eddy size, the eddy location within the 1D domain and the stirring frequency (event rate). The method to obtain these parameters is given elsewhere [12].

2.2 NUMERICAL IMPLEMENTATION OF LES MODEL

LES studies have been applied to methane-air flame studies [16-18] and to a generic combustor concept. Methane-air flames similar to those in the experiments [16-18] are studied here. In order to obtain a realistic chemical state over a wide range of operating conditions, a 15-step, 19-species skeletal mechanism is employed. This mechanism (which included No_x kinetics) has been shown to be quite accurate over a wide range of equivalence ratios. It is also capable of predicting extinction and re-ignition, which is particularly relevant here since F1 flame, is considered close to extinction limit. Table 1 summarizes the chemical species and reactions in this skeletal mechanism.

The numerical method is the same as in the earlier study [12] and therefore, only briefly summarized. To simulate a stationary flame, a moving observation window is used that translates with the flame brush to maintain approximately the same relative position between flame center and observation window (even though the flame propagates freely into the reactants). All statistics are obtained relative to the flame center. The computational domain is chosen large enough to fully capture this flame brush (typically $6L$). Earlier studies and the present study show that statistically, stationary flames can be simulated using this approach.

A fractional operator splitting method is used to first evolve (via molecular diffusion and turbulent stirring) the scalar equations (without the reaction terms) for a small time step δt to obtain the thermo-chemical state after mixing. Then the reaction

system is integrated over δt to get the final scales and hence, the computational cost for the time integration can be very high. Here, the ISAT approach is used to efficiently handle the finite rate kinetics.

In ISAT, only the accessed region of the composition space, which is a subset of the whole realizable region (the set of all possible combinations of compositions for a given number of species), is tabulated. This tabulation is done as a part of the simulation and when the same composition re-occurs, the table is searched and the stored information is retrieved using fast binary tree search algorithm. Since only the accessible region is stored, the overall time required to build, retrieve and store information reduces significantly. Further details of the ISAT algorithm is given elsewhere [13] and therefore, avoided here for brevity.

To further reduce computational cost, the present model was parallelized with message passing (needed for the solution of the reaction-diffusion equations) handled by MPI directives. For the chemistry point problem no communication is needed. Each processor builds a table for the composition that occurs inside its domain during the computation. This localizes the ISAT table to each processor and reduces the overall load (including search and retrieve time) for each processor (as opposed to building a single table for all the composition that occurs over the whole of the domain). All simulations were done on a 32 processor CRAY-T3E system.

Computational efficiency of ISAT is significant as reported earlier. The size of the table and cost depend upon the error tolerance (which determined the allowable error in each of the scalar for a given initial state). For higher accuracy, this parameter should be low, leading to an increase in the total simulations time and storage. For a value of ε_{tol} = 0.0008 a speed-up of around 30 in the chemical update is achieved by using ISAT. This is consistent with the speedup reported earlier. Table 2 summarizes the present results.

3. GOVERNING EQUATIONS FOR ONE-DIMENSIONAL COMBUSTION INSTABILITY MODEL

The combustor model numerically integrates the following governing differential equations for a calorically perfect gas. The governing equations are given below in non-dimensional form [9] as

$$\frac{\partial w}{\partial t}+\frac{\partial F(w)}{\partial x}=S \tag{1}$$

where the dependent vector w is given as

$$w=\begin{bmatrix} \rho \\ \rho u \\ \dfrac{p}{\gamma-1}+\dfrac{\rho u^2}{2} \\ \rho\ y_i \end{bmatrix} \tag{2}$$

and the flux vector is given by

$$F=\begin{bmatrix} \rho u \\ \dfrac{p}{\gamma}+\rho u^2 \\ u\left(\dfrac{p}{\gamma-1}+\dfrac{\rho u^2}{2}\right) \\ \rho\ u\ y_i \end{bmatrix} \tag{3}$$

The non-dimensionalization of pressure, p, temperature, T, density, ρ, and velocity, u has been obtained by using the reference quantities p^*, T^*, ρ^*, and a^*. The coordinate x has been scaled by the combustor length L. The time has been scaled using the sound wave transit time $t^* = L/a^*$. The heat of combustion q_0 is assumed to be a constant. The ratio of specific heats is denoted by γ.

The non-dimensional form of the equation of state is given as

$$p=\rho T \tag{4}$$

The source vector in Eq. (1) is given as

$$S=\begin{bmatrix} 0 \\ \dfrac{\partial}{\partial x}\left(\dfrac{\varepsilon_t}{\mathrm{Re}^*}\left(\dfrac{\partial u}{\partial x}\right)\right)+\sigma_2 u\left|\rho u\right|^{0.75} \\ \dfrac{\partial}{\partial x}\left(\dfrac{\varepsilon_t}{\mathrm{Re}^*}\dfrac{\partial}{\partial x}\left(\dfrac{u^2}{2}+\dfrac{p}{(\gamma-1)\,\mathrm{Pr}_t}\right)\right)+q_0 R+Q_{fh} \\ \dfrac{\partial}{\partial x}\left(\dfrac{\varepsilon_t}{\mathrm{Re}^*\,Sc_t}\left(\dfrac{\partial y_i}{\partial x}\right)\right)-R \end{bmatrix} \tag{5}$$

Equation (5) contains contributions from the reaction, turbulent eddy diffusion, wall viscous forces, and flameholder heat transfer. The Reynolds number, Re^* is defined as $\rho^* a^* L/\mu$. The

turbulent viscosity ratio, ε_t is defined as the ratio of turbulent to molecular viscosity, μ_t/μ. R is the reaction rate, defined below. Pr_t and Sc_t are the turbulent Prandtl and Schmidt numbers respectively.

3.1 COMBUSTION MODEL FOR ONE-DIMENSIONAL COMBUSTION INSTABILITY MODEL

The combustion model employed in this study was based upon a single-step chemistry reaction scheme. The non-dimensional reaction rate has the form:

$$R = K_0 \rho\, y_f\, y_{o_2} \begin{Bmatrix} 1-\left(T_{ign}/T_i\right) & ;T_i > T_{ign} \\ 0 & ;T_i < T_{ign} \end{Bmatrix} \qquad (6)$$

where K_0 is the reaction rate constant, T_{ign} is the ignition temperature and T_i is the temperature in the i^{th} numerical cell. Due to the one-dimensionality of the combustor model, flame holding is accomplished by a 10% change of the ε_t over the combustor length from zero to a specified value.

3.2 FLAMEHOLDER HEAT TRANSFER FOR ONE-DIMENSIONAL COMBUSTION INSTABILITY MODEL

The term Q_{fh} in Eq. (5) is represented by a simple algebraic expression

$$Q_{fh} = \alpha(0.9T_{ign} - T_i^{fh}) \qquad (7)$$

where α is a user specified constant, $0.9T_{ign}$ represent the assumed temperature of the flameholder to or from which heat may be transferred, and T_i^{fh} is the (computed) gas temperature at the flameholder location. Note that when this model is used, energy is not strictly conserved in the system. That is, energy may be brought into or taken from the system by this term. T_{ign} is assumed to be constant, since the flame response time scale is much smaller than that of the flameholder wall temperature.

3.3 NUMERICAL METHODOLOGY FOR ONE-DIMENSIONAL COMBUSTION INSTABILITY MODEL

The combustor model numerically integrates the above equations of motion using a very simple, second-order MacCormack scheme. Artificial viscosity has been added in order to damp non-physical oscillations in the vicinity of strong gradients such as those brought about by the combustion process [19-22]. A number of grid independent studies were conducted to ensure that physical instability would not be damped [22]. In the current study, the grid size was $\Delta x = 0.005$ mm for which the results were very much grid-independent, as will be shown in the results.

3.4 BOUNDARY CONDITIONS FOR ONE-DIMENSIONAL COMBUSTION INSTABILITY MODEL

Boundary conditions may be imposed as either partially opened, fully open, or choked inflow (e.g. constant mass flux) ends. In either case the model anticipates the flow direction and applies appropriate (e.g. well posed) states. If the flow is outward from the computing domain, only the static pressure is imposed. The remaining information, density, velocity, and mass fraction are obtained from the interior of the computational domain. If the flow is inward, total pressure and temperature, and mass fraction are imposed. The remaining unknown quantities (velocity, static temperature and pressure) are obtained through an iteration procedure by using isentropic relations for static and total temperature and pressure. In other words, the velocity is first obtained by using $\partial u/\partial x = 0$ at the exit. Then, the static temperature is obtained iteratively through the relation $T_o/T = 1 + 0.5(\gamma - 1)u^2/(\gamma RT)$. Finally, the static pressure is obtained through p_o/p_t relation.

4 RESULTS

In this part of the study, efforts were mainly focused on demonstrating the uncombined performance of the one-dimensional combustor model and the LES methodology in suitable combustor configurations. The objective here is to provide confidence that the two models are capable of predicting the reaction flow field. In sequent study Part II, the information obtained from LES will be used to guide the application of the one-dimensional model in a combined manner. Results obtained from the one-dimensional combustor model will be first presented, followed by the results obtained from LES respectively.

4.1 ONE-DIMENSIONAL RESULTS

Numerical results have been obtained to demonstrate the applicability of the unsteady one-dimensional combustor model to predict combustion-driven instability in a generic gas turbine combustor. Figure 1 shows the schematic of the combustor geometry investigated in this study. Fully premixed fuel-air mixture was assumed at the inlet of the combustor. The fuel

type used was JP-8. Combustor model constants used in this study are given in Table 3. As indicated earlier, two different types of exit boundary conditions were implemented in the combustor model, namely, full open and choked. In this preliminary study, only the open exit boundary condition was used. The boundary condition imposed at the exit corresponds to a non-dimensional pressure value of unity. In fact, the reference pressure in this study was assumed to be equal to the back pressure. Due to the one-dimensionality of the combustor model, the effects of the swirl velocity component was accounted for by using a 1.1 % reduction in the static pressure at the combustor inlet.

The combustor model assumes that a constant fuel-air flux can be specified at the inlet in the absence of combustor pressure acoustics. This condition is essentially a choked boundary in which the effect of the downstream pressure acoustics are not sensed upstream of the inlet. However, a choked inlet condition would lead to stable combustion as the computations showed. The dependence of the inlet fuel-air mixture flux upon the combustor pressure should, therefore, be determined through a fuel injection system model. Since the current study assumes the computational domain to start at the backward facing step, a lumped-element parameter model for the fuel injectors/swirlers was considered.

$$\dot{m}_2 = \dot{m}_1 - \frac{\rho V}{k}\frac{dp'}{dt} \tag{8}$$

Equation (8) expresses the dependence of the fuel-air flow rate at the inlet of the combustor, $\dot{m}_2$, on the combustor pressure oscillations p'. The fuel-air mixture mass flow rate $\dot{m}_1$ is a constant. Equation (8) also implies that as the combustor pressure oscillation $p' \to 0$, $\dot{m}_2 = \dot{m}_1$ and a constant fuel-air mixture flow rate is then imposed at the combustor inlet.

The location of the fuel injection and the time required for the fuel-air mixture to react are very critical parameters for either driving or damping the instabilities [6,7]. The time delay between the instant of fuel injection and the instant of heat release is primarily governed by the mixing and chemical kinetic times. To account for this time delay, various estimations of this time delay were made based on the location of the fuel injector and chemical times for different equivalence ratios (i.e., ϕ = 0.5 - 0.8), initial temperatures (i.e., T_{inlet} = 700 - 900 K) and Damkohler numbers (Da = 1.0 - 100). The time delay was then used in the combustor model to determine the instant at which the fuel-air mixture, $\dot{m}_1$, is injected. The resultant mixture injection was therefore shifted in time by an amount equal to the time delay (i.e., injection time = $t \pm \delta t$) and $\dot{m}_1(t \pm \delta t)$ is injected.

Figures 2 and 3 show the combustor limit cycle pressure oscillations and the corresponding heat release in non-dimensional form and for a time delay of 1.97×10^{-3} s and at a non-dimensional location x = 0.8. This value of the time delay was found to produce the largest amplitude of the pressure oscillations. The cycle limit pressure oscillations have a non-dimensional period of approximately 0.9 (or 3.6×10^{-3} s) and a corresponding non-dimensional frequency of 1.11 (or 278 Hz). It can also be seen that these strong oscillations have shock waves characteristics, which indicate that these are a strong longitudinal instability of the fundamental mode 278 Hz. In addition, a close examination of the limit cycle pressure oscillations and that of the heat release fluctuations clearly exhibits the phase relationship between the heat release and the pressure oscillations. Pressure and heat release oscillations were predicted to be in phase and thus satisfy Rayleigh's criterion for driving instability.

Figure 4 shows the pressure field oscillations for a time delay of 3.8×10^{-3} s which is equal to 1.97×10^{-3} + half the limit cycle period shown in Fig. 2. It is clearly seen that the strong limit cycle oscillations of Fig. 2 have been substantially damped, consistent with the time lag theory of Crocco [23]. This demonstrates the capability of the combustor model to simulate non-linear behavior. Additional simulations were carried out to substantiate the time delay effect and the results were all consistent. It should be mentioned that when calculations were made for constant fuel-air mixture mass flow rate (time delay and p' are set equal to zero), a steady-state combustion was predicted.

To further demonstrate the ability of the combustor model to carry out active control calculations, the combustor response to fuel flow modulation as a means to actively control instability was predicted. The fuel injection was pulsed sinusoidally at different frequencies and amounts. The predictions represent the open loop response of the controlled combustor as shown in Fig.1. Note here that no phase shift and controller gain were used in the current study. The inlet condition for the open loop calculations was set to be a constant fuel-air mixture flux with various time delays (i.e., non-choked inlet) and the exit condition was also open with a specified non-dimensional pressure of unity. The combustor length was also kept the same to ensure that the combustor resonant frequencies are considerably higher than the fuel pulsation frequencies. The amplitude of the amount of fuel pulsed was varied between 2% to 10% of the total primary fuel injection rate and the combustor response was studied.

Figures 5-8 show the predicted combustor response in terms of the non-dimensional pressure, temperature, velocity

and primary fuel mass fraction for a time delay of 1.97×10^{-3} s and at the non-dimensional location x = 0.8. The non-dimensional fuel pulsation frequency ω was 0.6 (i.e., ω = 150 Hz) and the non-dimensional magnitude A was 2% of the primary fuel rate. The sinusoidal fuel pulsation was turned on at the start of the computations (i.e., after one computational time step for convergence and code stability). The results clearly show that significant damping of the pressure, temperature and velocity oscillations occurred. In particular, it can be seen that the pressure initially increases due to the rapid rise in the temperature and then it is followed by a period over which the pressure oscillates and finally the oscillations damp out. This behavior is also reflected in temperature and velocity fields.

Figures 9 and 10 show the non-dimensional pressure and temperature in the combustor for A = 10% of the primary fuel rate and for the same conditions as in Figs. 5 through 8. It can be seen that increasing the amount of pulsed fuel does not always result in more damping. In fact, the amplitude of the final oscillations appear to be somewhat greater than that of the previous case, for A = 2%. However, the increase in the oscillation magnitude is not significant.

To further study the effect of fuel pulsation on the combustor response, the fuel pulsation was turned on after the limit cycle pressure oscillations were reached for the case presented in Figs. 2 and 3. The combustor response predictions are shown in Figs. 11-13. It is clearly demonstrated that if the fuel is pulsed after the system has reached a limit cycle, the decrease in the amplitude of the pressure oscillations appears to be limited and never goes to zero as the computations revealed. The reason for this behavior may be attributed to the inability of pulsed fuel to produce a secondary heat release oscillation of sufficient amplitude and be completely out of phase with the strong limit cycle pressure oscillations. This can further be seen in Fig. 11 where the heat release fluctuations are not entirely out of phase with the pressure oscillations. It should also be indicated that a similar behavior was seen [5], when an active control was turned on after the system has reached the limit cycle behavior. This is indicative of the unsatisfactory performance of fuel pulsation to control instability in the limit cycle regime. Multiple fuel pulsation frequencies based on multiple pressure modes sensed in the combustor will be required to damp non-linear instabilities, which will be investigated in the near future.

4.2 LES OF TRAPPED VORTEX COMBUSTOR

The TVC is a combustor design under investigation for IHPTET applications. In this concept, the combustion occurs in a vortex trapped within a cavity and past results suggests that this can increase flame stability. Figure 14 shows schematically, the combustor simulated in the present study.

Various studies into the application of cavity-flow interaction have been conducted in the past. Earlier [24] it was noted that a cavity-locked vortex entrains very little main-flow air and would result in a low exchange of mass and heat between the cavity and the main flow, Since combustion requires a continuous supply of reactants, fuel and air must be directly injected in the cavity to sustain the burning processes. However, direct injection (mass addition) can disrupt the flow dynamics, possibly resulting in cavity instability. Previous attempts at numerical modeling of TVC [25, 26], noted the possibility of mixing-limited reactions in the TVC. For this reason, fuel/air mixing and its effect on combustion in the TVC is investigated in this study.

The model formulation and the various closure models are summarized in a recent paper [27] and therefore, not repeated here. In the following, we briefly highlight some of the salient features observed in this study.

To investigate the fluid dynamic mixing properties of the TVC, two cases (I & II) were conducted under identical conditions except that the air velocity at the inlet was changed from 20 m/s (case I) to 40 m/s (case II). Non-reacting mixing was studied with fuel is injected into the cavity with an equivalence ratio far above stoichiometric (ϕ = 4.4). Thus, entrainment and mixing with the ambient air is critical in order to achieve efficient combustion.

To increase mixing rates, higher turbulence levels are also desired. Regions of high mean and, perhaps more importantly, high RMS velocities will tend to enhance mixing rates. Therefore, we investigated the effect of increasing in the primary airflow rate.

For visualization, the time averaged and instantaneous velocity vectors for cases I & II are shown in Figs. 15(a) & 15(b), respectively. The higher annular flow rate (Fig. 15(b)) enhances the trapped-vortex strength, allowing for increased annular/cavity flow interaction. In the time averaged results, it is seen that two vortices are present for case I. In addition to a vortex rotating in the direction of the annular flow, the second vortex rotates in the reverse direction. However, these vortices are not observed in case II. Rather, only a single, large vortex rotates with the flow. The instantaneous images on the other hand do show transient vortices in the shear layer and in the cavity indicating a process of unsteady entrainment of the primary air from the inlet. As discussed elsewhere [27] and noted below, this turbulent mixing appears to be beneficial for fuel-air mixing.

Two reacting-flow cases (IV & V) were also used to investigate the impact of fuel/air mixing rates under reacting conditions. The primary equivalence ratio of the cavity jets in both cases was again 4.4 and the injection temperature was a slightly elevated value of 500 K. As observed by Sturgess et al.

[28], the cavity flow entrains relatively little annulus air and will tend to be fuel-rich under reacting flow conditions. This was confirmed by looking at the mean fuel and oxygen mass fractions [27] (not shown here). For the low speed case, near the injection ports, the RMS values are much higher due to fluctuations in velocity and species composition. Far from the injectors, however (near the fore-body wall), the oxygen is almost entirely consumed leaving a fuel-rich cavity region. The remaining fuel is finally consumed outside the cavity in either the dump shear layer or downstream of the after-body, depending on the inlet flow velocity. For the higher flow velocity, on the other hand, more fuel is consumed in the cavity. This indicates that the primary air stream is entrained more with increase in flow velocity and the increase turbulence enhances fine-scale mixing.

The rate at which the fuel is mixed can be viewed by examining the species mixture fraction, Z, as a function of inflow velocity. Shown in Figs. 16(a) and 16(b) are the instantaneous and time averaged stoichiometric mixture fraction surfaces, $Z = Z_{st}$, for both reacting flow cases (The stoichiometric surface, Z_{st}, has been highlighted by a single black line, where Z_{st} for methane air is approximately 0.055). As can be seen in Fig. 16(b) (U_o = 40 m/s), Z_{st} is almost entirely contained inside the cavity region for both the instantaneous and the time averaged results. For the lower inflow velocity, the surface extends far downstream of the cavity zone.

Also shown in Figs. 16(a) and 16(b) are the instantaneous and time-averaged temperature color contours for cases IV & V. Following the same trends as Z, the peak temperature regions are seen to shift from outside the cavity region for a lower annular velocity to inside the cavity in case V. In both mean and instantaneous views, the cavity temperature increases with increases flow velocity.

Comparisons with experimental data is possible for case V. The mean and RMS temperature profiles reported by Hsu et al. [24] (obtained with CARS technique) are super-imposed in Fig. 17. The combustor conditions were nearly identical to those simulated in case V, U_o = 42 m/s, ϕ = 4.4, H/d = 0.59: however, propane instead of methane was used as the primary fuel. Despite this difference, the mean temperature trends should still be comparable. A maximum instantaneous temperature of 2025 K was obtained inside the cavity in case II which is slightly lower then the 2150 K reported by Hsu et al [24].

For both inflow velocities, the mean temperature near the injection ports has not been greatly effected. However, away from the injectors, the higher inflow velocity resulted in higher cavity temperatures for both mean and instantaneous profiles. The peak temperature region for the case IV is not inside the cavity but downstream in the after-body wake resulting in longer thermal residence times. The longer residence times may increase thermal No_x production. As would be expected with the higher inflow velocity, the downstream temperature is lower despite higher cavity temperatures. This is mainly due to the higher volume flow rate and lower overall equivalence ratio. The combination of a higher fuel consumption rate and higher velocity results in a lower thermal residence time. This is beneficial to lower combustion pollutant formation.

5 CONCLUSION

Large eddy simulation and one-dimensional analysis were carried out to predict combustion-driven dynamic instabilities. The one-dimensional combustor model was first used to study active control of combustion-driven instabilities in a generic gas turbine combustor. The numerical predictions clearly demonstrated the effect of the time delay between the instant of fuel injection and heat release. By varying this time delay, damping or driving of the instability may occur. The predictions showed that there existed a single time delay value for the combustor geometry considered here and for which strong instability can set out and is manifested by a limit cycle behavior. The analysis also showed that these strong pressure oscillations can be damped out by changing the delay time by some factor multiplied by the oscillation period.

The one-dimensional combustor model was also used to investigate the combustor response to fuel flow pulsation to control instability. The results clearly demonstrated that for fuel pulsation to be effective in controlling instability, the fuel modulation must be turned on at the start of the engine. Moreover, the results indicated that multiple frequency-based fuel pulsation might be required to damp out strong shock wave type instability oscillations.

The use of In-situ Adaptive Tabulation (ISAT) to efficiently calculate multi-species finite-rate kinetics is demonstrated in this study. It is also demonstrated that the LEM model can be used to simulate premixed combustion regardless of the nature of the flame structure (i.e., flamelet or thin-reaction-zones) without requiring any ad hoc fixes. This study when combined with the earlier studies clearly suggest that subgrid combustion modeling for LES is a viable option even when finite-rate kinetics is to be simulated.

Finally, it should be mentioned that the combustor model developed here is a very useful predictive tool that can be used during the predesign and design stages to predict the dynamic instability characteristics of new combustor designs in a very efficient manner. However, detailed description of the unsteady flow field must be predicted in order to use the one-dimensional model to suppress combustion-driven dynamic instabilities.

ACKNOWLEDGMENTS

The authors would like to thank Dr. Paxson from NASA Glenn Research Center for the technical discussion and providing us with the original baseline code for one-dimensional combustor model. The LES work was supported by the Army Research Office under the Multidisciplinary University Initiative.

REFERENCES

1. Darling, D., Radhakrishnan, K., Oyediran, A., and Cowan, E., "Combustion-Acoustic Stability Analysis for Premixed Gas Turbine Combustors," NASA TM 107024.
2. Bloxsidge, G. J., Dowling, A. P., and Langhorne, P. J., "Reheat Buzz: an Acoustically Coupled Combustion Instability. Part 2. Theory," *J. Fluid Mech.*, Vol. 193, pp. 445-473, 1988.
3. Bloxsidge, G. J., Dowling, A. P., and Langhorne, P. J., "Active Control of Reheat Buzz," *AIAA Journal*, Vol. 26, No. 7, pp. 783-790, 1988.
4. Shyy, W. and Udaykumar, "Numerical Simulation of Thermo-Acoustic Effect on Longitudinal Combustion Instabilities," 26th JPC, *AIAA 90-2065*, 1990.
5. Mohanraj, R. and Zinn, B. T., "Numerical Study of the Performance of Active Control Systems for Combustion Instabilities," 36th JPC, *AIAA 98-0356*, 1998.
6. Smith, C.E., and Leonard, A., D. "CFD Modeling of Combustion Instability in Premixed Axisymmetric Combustors," *ASME Paper 97-GT-305*, 1997.
7. Habiballah, M. and Dubois, I., "Numerical Analysis of Engine Instability," 31st JPC, *AIAA 95-37213*, 1995.
8. Kim, Y. M., Chen, C. P., Ziebarth, J. P., and Chen, Y. S., "Prediction of High Frequency Combustion Instability In Liquid Propellant Engines," 28th JPC, *AIAA 92-3763*, 1992.
9. Quinn, D., D and Paxson, D. E., "A Simplified Model for the Investigation of Acoustically Driven Combustion Instability," 34th JPC, *AIAA 98-3764*, 1998.
10. Hsiao, G., Pandalai, R., Hura, H., and Mongia, H. C., "Combustion Dynamic Modeling for Gas Turbine Engines," 34th JPC, *AIAA 98-3380*, 1998.
11. Yang, V., and Anderson, W., "Liquid Rocket Engine Combustion instability," *Progress in Astronauts and Aeronautics*, Vol. 169, 1995.
12. Menon, S., Kim, W.-W., Stone, C., and Sekar, B., "Large-Eddy Simulation of Fuel-Air Mixing and Chemical Reactions in Swirling Flow Combustor," *AIAA 99-3440*, 30th Plasma Dynamics and Lasers Conference, Norfolk, VA, June 1999.
13. Menon, S., Stone, C., Sankaran, V., and Sekar, B., "Large-Eddy Simulations of Combustion in Gas Turbine Combustors," *AIAA 00-0960*, Jan. 2000.
14. Kim, W.-W. and Menon, S., "A New Incompressible Solver for Large-Eddy Simulations," *International Journal of Numerical Fluid Mechanics*, Vol. 31, pp. 983-1017, 1999.
15. Kerstein, A. R., "Linear-Eddy Model of Turbulent Transport II," *Combustion and Flame*, Vol. 75, pp. 397-413, 1989.
16. Chen, Y., Peters, N., Schneemann, G., Wruck, N., Renz, U., and Mansour, M., "The Detailed Structure of Highly Stretched Turbulent Premixed Methane-Air Flames," *Combustion and Flame*, Vol. 107, pp. 223-244, 1996.
17. Mansour, M., Peters, N., and Chen, Y., "Investigation of Scalar Mixing in the Thin Reaction Zones Regime Using a Simultaneous CH-LIF/Rayleigh Laser Technique," *Twenty-Seventh Symposium (International) on Combustion*, pp. 767-773, 1998.
18. Bedat, B. and Cheng, R. K., "Experimental Study of Premixed Turbulent Flames in Intense Isotropic Turbulence," *Combustion and Flame*, Vol. 100, pp. 486-494, 1995.
19. Paxson, D. E., "A General Numerical Model for Wave Rotor Analysis," NASA TM 105740, July 1992.
20. Paxson, D. E., "An Improved Numerical Model for Wave Rotor Design and Analysis," *AIAA 93-0482*, Jan. 1993, also NASA TM 105915.
21. Paxson, D. E., "A Comparison Between Numerically Modeled and Experimentally Measured Loss Mechanisms in Wave Rotors," *AIAA Journal of Propulsion and Power*, Vol. 11, No. 5, 1995, pp. 908-914, also NASA TM 106279.
22. Nalim, R. M. and Paxson, D. E., "A Numerical Investigation of Premixed Combustion in Wave Rotors," *ASME Journal of Engineering for Gas Turbines and Power*, Vol. 119, No. 3, 1997, pp. 668-675, also ASME Paper 96-GT-116, June, 1996, also, NASA TM 107242.
23. Crocco, L. and Cheng, S.-I., "Theory of Combustion Process Instability in Liquid Rocket Engines," IL, Moscow, 1958, pp. 59-69.
24. Hsu, K.-Y., Goss, L. P., and Roquemore, W. M., "Characteristics of a Trapped-Vortex Combustor," *Journal of Propulsion and Power*, Vol. 14, No. 1, pp. 1-12, 1998.
25. Katta, V. and Roquemore, W., "Numerical Studies on Trapped-Vortex Combustor," *AIAA 96-2660*, 1996.
26. Katta, V. and Roquemore, W., "Study of Trapped-Vortex Combustor – Effect of Injection on dynamics of Non-Reacting and Reacting Flows in a Cavity," *AIAA 97-3256*, 1997.
27. Stone, C. and Menon, S., "Simulation of Fuel-Air Mixing and Combustion in a Trapped Vortex Combustor," *AIAA 00-0478*, 2000.
28. Sturgess, G. and Hsu, K.-Y., "Entrainment of Mainstream Flow in a Trapped-Vortex Combustor," *AIAA 97-0261*, 1997.

Table 1 15 Step, 19 Species Mechanism

$H + 0.5O_2 = OH$
$H_2 + 0.5O_2 = H + OH$
$HO_2 = 0.5O_2 + OH$
$0.5O_2 + H_2O_2 = OH + HO_2$
$0.5O_2 + 0.5C_2H_2 = H + CO$
$CH_3 + CO + C_2H_4 = 0.5O_2 + CH_4 + 1.5C_2H_2$
$0.5O_2 + 2CH_3 = H_2 + CH_4 + CO$
$0.5O_2 + CH_3 = H + CH_2O$
$0.5O_2 + CH_4 = OH + CH_3$
$0.5O_2 + CO = CO_2$
$0.5O_2 + C_2H_6 = CH_4 + CH_2O$
$H + OH = H_2O$
$H + CH_4 + NO + HCN = 0.5O_2 + 2CH_3 + N_2$
$H + 0.5O_2 + CH_4 + HCN = 2CH_3 + NO$
$0.5O_2 + CH_4 + NH_3 + HCN = H_2O + 2CH_3 + N_2$

Table 2 ISAT Performance

	ϵ_{tol} = 5E-3	ϵ_{tol} = 8E-3	*DI*
Total CPU time	16.66 h	9.46 h	31.11 h
Chemistry time	0.0108 s	7.3e-3 s	0.2278 s
Speed up in Chemistry	21	31	-
Speed up in simulation	2	3	-
No. of Records	40500	16500	-

Table 3

Model Constants	
γ	1.37
ε_t	0.002
Sc_t	1.0
Pr_t	1.0
T_{ign}	1.25

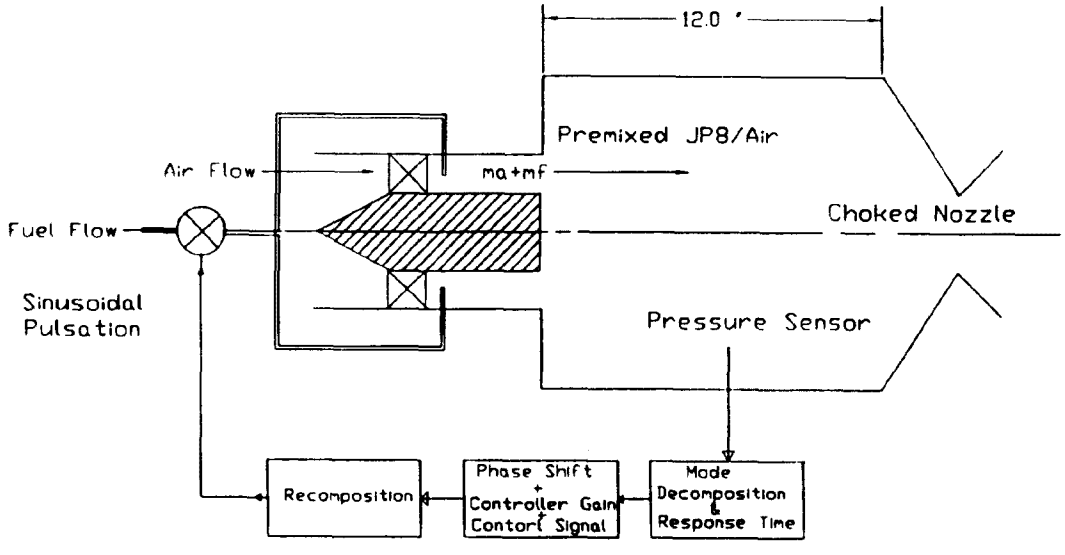

Fig. 1 A Schematic of the Combustor and Control System.

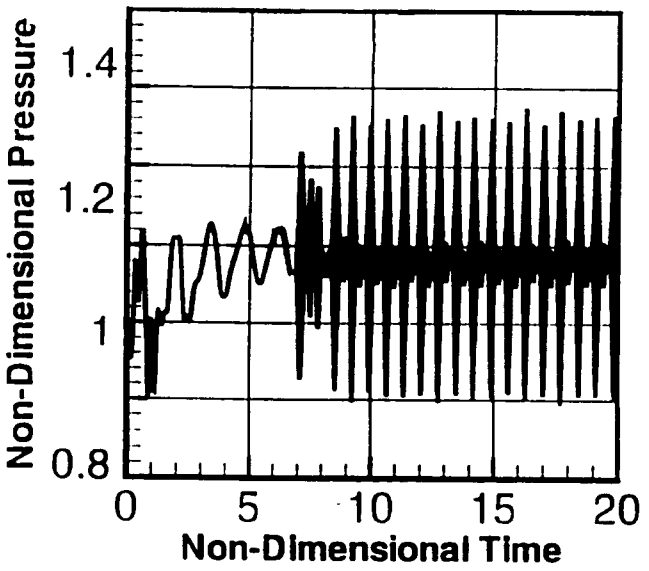

Fig. 2 Limit Cycle Pressure Oscillations for a Time Delay $\delta t = 1.97 \times 10^{-3}$ s.

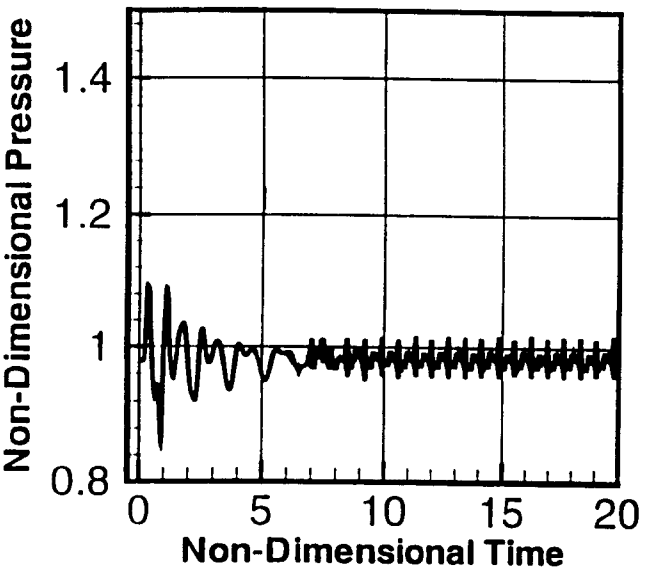

Fig. 4 Effect of Time delay on the Limit Cycle Pressure Oscillations for a Time Delay $\delta t = 1.97 \times 10^{-3} + 1.8 \times 10^{-3}$ s.

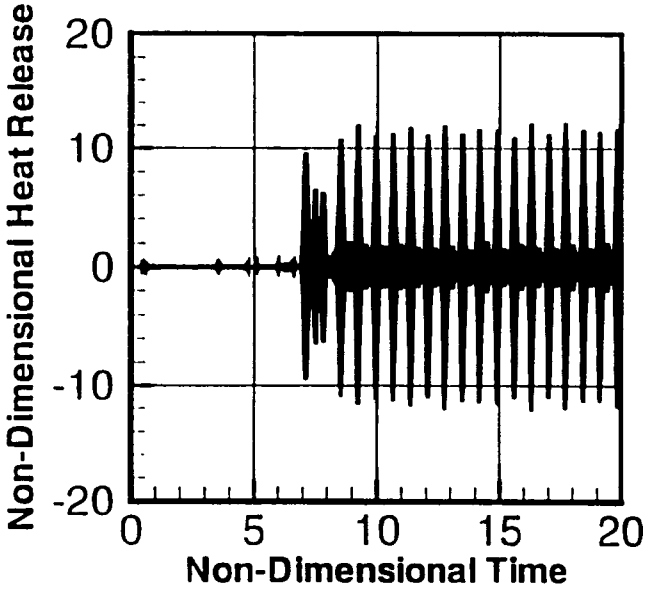

Fig. 3 Non-Dimensional Limit Cycle Heat Release Oscillations Corresponding to $\delta t = 1.97 \times 10^{-3}$ s.

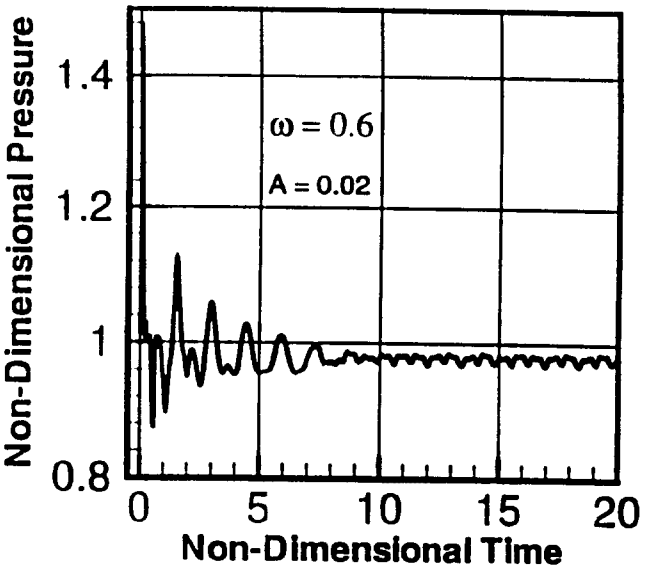

Fig. 5 Effect of Fuel Modulation on the Pressure Oscillations for Concurrent Primary and Pulsed Fuel Injection.

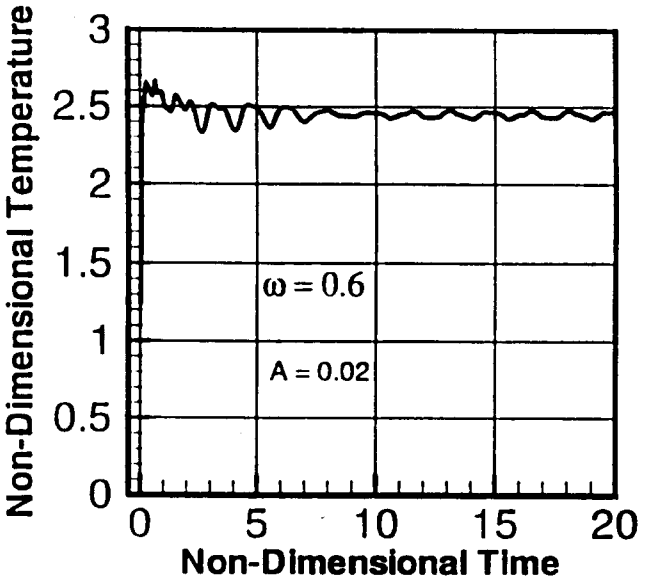

Fig. 6 Effect of Fuel Modulation on the Temperature Oscillations for Concurrent Primary and Pulsed Fuel Injection.

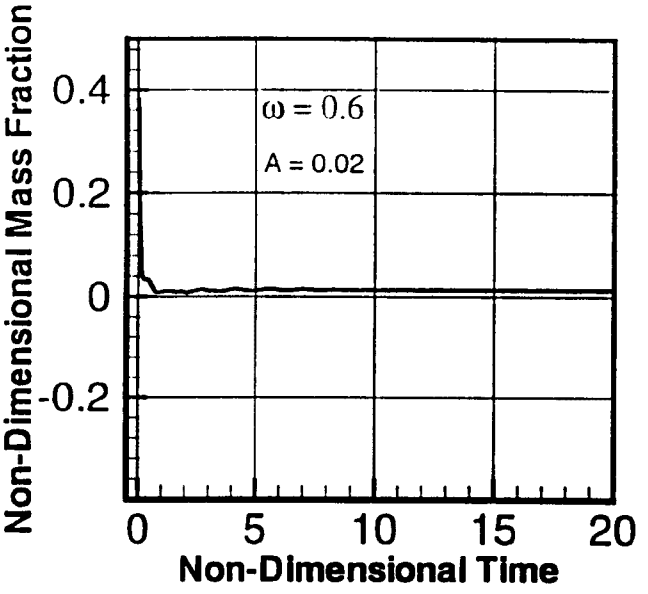

Fig. 8 Effect of Fuel Modulation on the Fuel Concentration Oscillations for Concurrent Primary and Pulsed Fuel Injection.

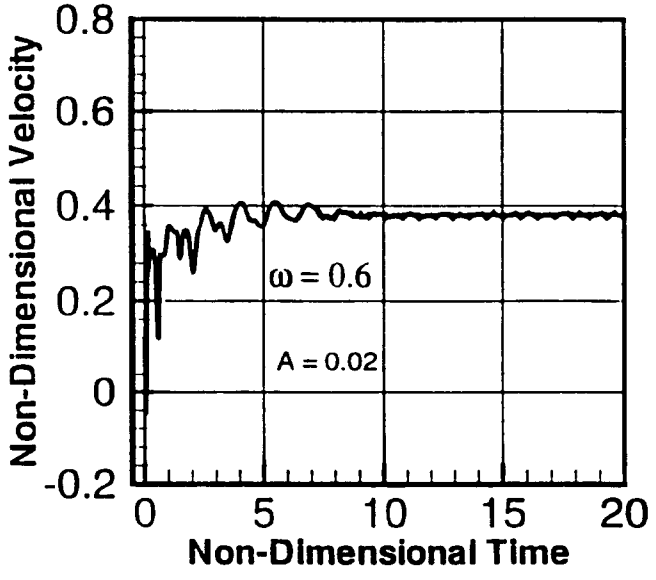

Fig. 7 Effect of Fuel Modulation on the Velocity Oscillations for Concurrent Primary and Pulsed Fuel Injection.

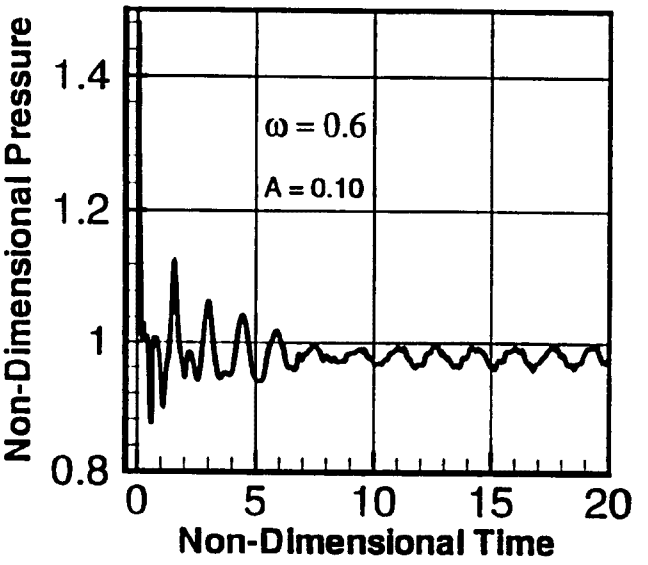

Fig. 9 Effect of the Amount of Fuel Modulation on the Pressure Oscillations for Concurrent Primary and Pulsed Fuel Injection.

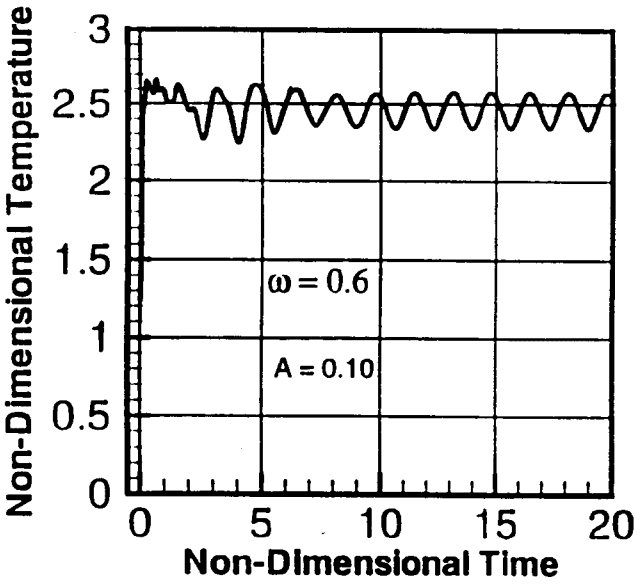

Fig. 10 Effect of the Amount of Fuel Modulation on the Temperature Oscillations for Concurrent Primary and Pulsed Fuel Injection.

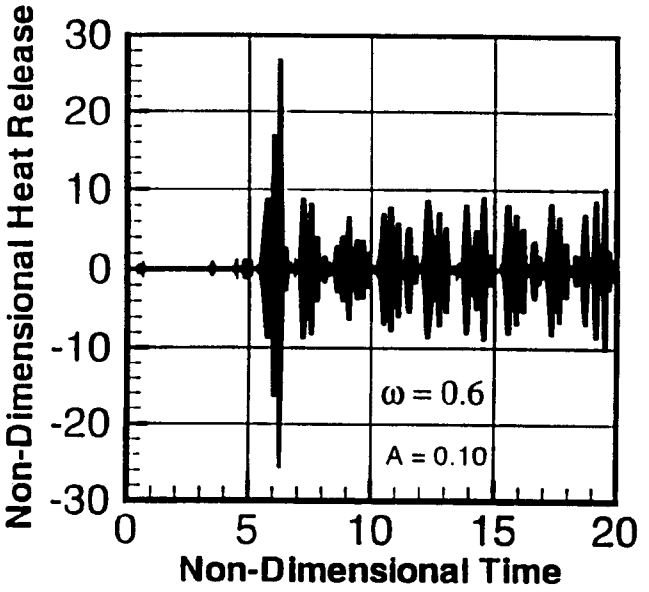

Fig. 12 Effect of Fuel Modulation on the Limit Cycle Heat Release Oscillations for Non-Concurrent Primary and Pulsed Fuel Injection.

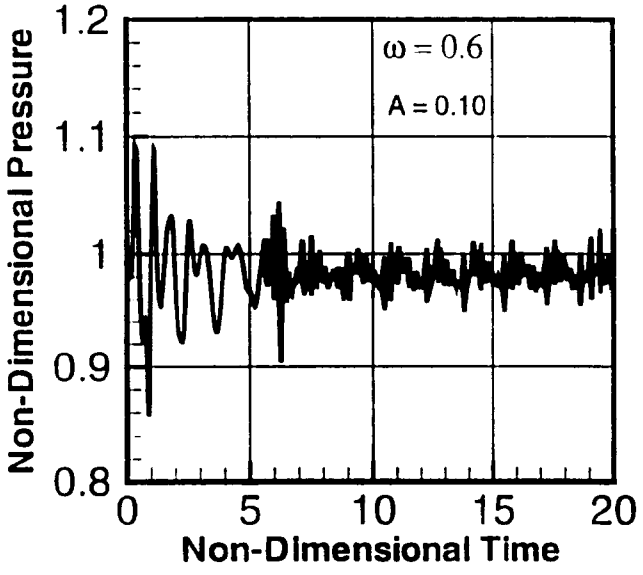

Fig. 11 Effect of Fuel Modulation on the Limit Cycle Pressure Oscillations for Non-Concurrent Primary and Pulsed Fuel Injection.

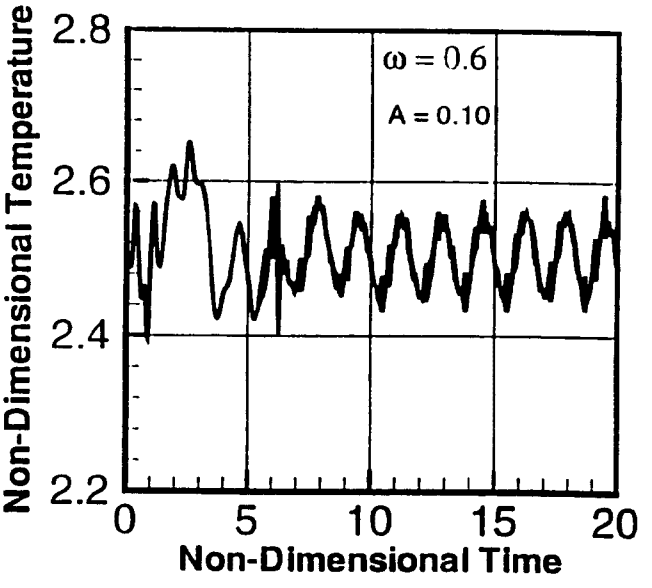

Fig. 13 Effect of Fuel Modulation on the Limit Cycle Temperature Oscillations for Non-Concurrent Primary and Pulsed Fuel Injection

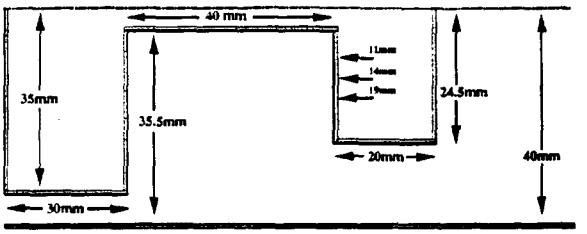

Fig. 14 Trapped-Vortex Geometry Used in This Numerical Study. Total Length (x) = 285 mm.

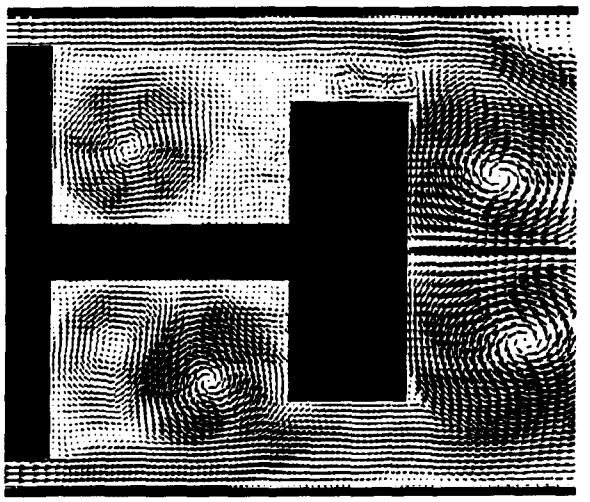

a) U_o = 20 m/s

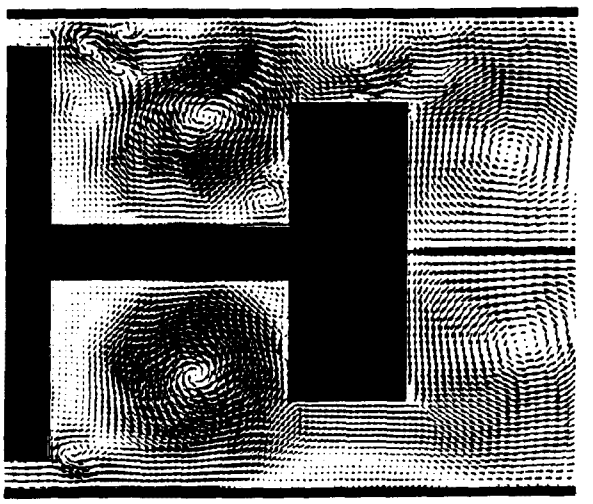

b) U_o = 40 m/s

Fig. 15 Non-Reacting Velocity Vectors for U_o = (a) 20 m/s, (b) 40 m/s (cases I & II). Upper Halves are Instantaneous, Lower Halves Are Time Averaged.

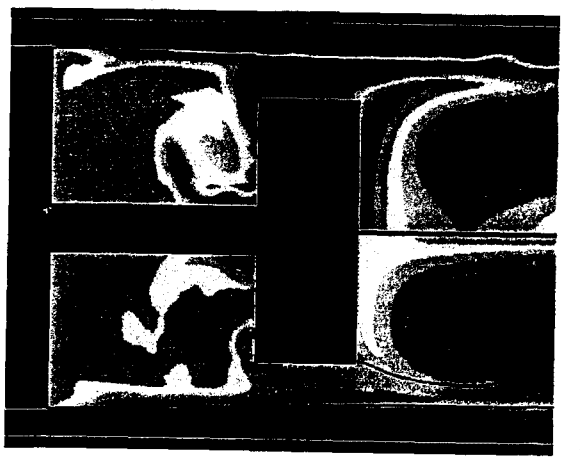

a) U_o = 20 m/s

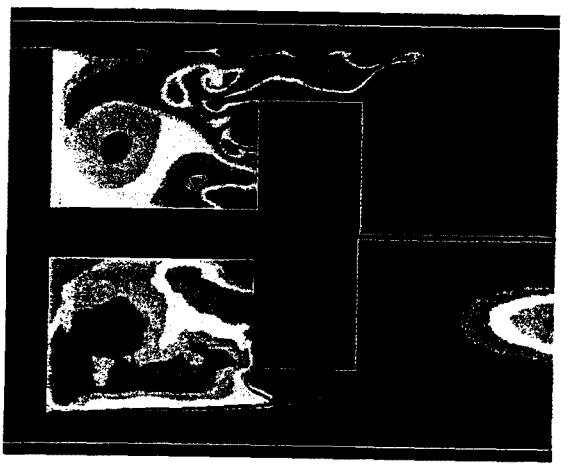

b) U_o = 40 m/s

Fig. 16 Reacting Flow Temperature Field and Stoichiometric Surface for U_o = (a) 20 m/s, (b) 40 m/s. Upper Halves are Instantaneous, Lower Halves Are Time Averaged. Temperature Color Contour Ranges Are 300 K (Blue) and 2000 K (Red). Stoichiometric Mixture Fraction, Z = $Z_{st} \cong 0.055$, Shown with Black Line.

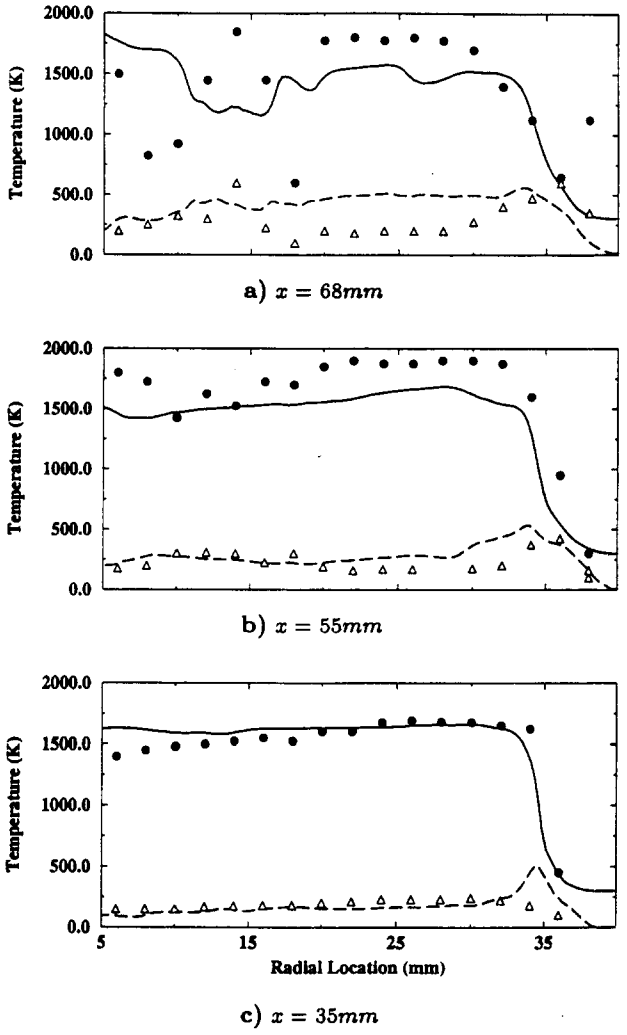

Fig. 17 Mean and RMS Temperature Profiles at x = (a) 68, (b) 55, (c) 35 mm for U_0 = 40 m/s (Case V).
$< \widetilde{T} >$ (—), $\widetilde{T}^{RMS}$ (– –), T_{exp} (•), T_{exp}^{RMS} (Δ).
Experimental results ($_{exp}$) from Hsu *et al.*

PAPER -19, B. Sekar

Question (J.-P. Hathout, USA)

According to the authors, pulsing in open loop causes the "unstable" system to become "stable". Can the author clarify the physics behind this behavior? Can it be inferred from the dynamics of the model what type of nonlinearities are responsible for stability?

Reply

The idea is, when the system is unstable, it could be damped by giving a frequency and modulating a portion of the fuel to different amplitude magnitude. But totally this cannot be made to be stable. There will still be oscillations, but either reduced or amplified depending on the frequency or amplitude. Thus, you could change the oscillating pattern and magnitude by different input of either the time delay or frequency or amplitude. The nonlinearities to predict the limit cycle behavior comes from time dependent boundary conditions, time dependent formulation of the basic equations, and the coupling of unsteady pressure fluctuations and the fuel-air oscillations.